Balancing osteogenesis and adipogenesis in osteogenesis imperfecta: *PLIN2* and *E2F2* as key targets for mesenchymal stem cell therapy

Xishun Wang[C,D,F], Zhenjiang Liu[A–C,E,F], Xinyong Hu[B,C,E,F], Yinpeng Cui[B,C,E,F]

Department of Orthopedics, Capital Center for Children's Health, Capital Medical University, Beijing, China

A – research concept and design; B – collection and/or assembly of data; C – data analysis and interpretation;
D – writing the article; E – critical revision of the article; F – final approval of the article

Advances in Clinical and Experimental Medicine, ISSN 1899–5276 (print), ISSN 2451–2680 (online) *Adv Clin Exp Med*. 2026;35(5):835–846

Address for correspondence
Xishun Wang
E-mail: wangxishun96@163.com

Funding sources
None declared

Conflict of interest
None declared

Received on April 27, 2025
Reviewed on July 7, 2025
Accepted on July 31, 2025

Published online on May 26, 2026

Abstract

Background. Osteogenesis imperfecta (OI) necessitates innovative mesenchymal stem cell (MSC) therapies targeting key molecular pathways to enhance targeted and combination treatments and improve bone health.

Objectives. To investigate the therapeutic mechanisms of various interventions for OI by analyzing relevant datasets, with a focus on lipid metabolism-related genes, particularly *PLIN2*, in order to determine whether they influence the balance between osteoblast and adipocyte differentiation.

Materials and methods. This study analyzed datasets from the Gene Expression Omnibus (GEO; GSE157587, GSE214064, GSE186141) and UK Biobank genome-wide association study (GWAS) summary statistics (UKB-b-4657, UKB-b-1096, UKB-b-8875, UKB-b-20124) using bioinformatics tools, including GEO2R, DESeq2, TwoSampleMR, MR-Egger, MR-PRESSO, gwasrapidd, and summary data-based Mendelian randomization (MR), to identify differentially expressed genes (DEGs) and assess causal relationships with heel bone mineral density (BMD).

Results. Differentially expressed genes analysis of GSE157587 identified *PLIN2* as the most significant gene influenced by MSC therapy in OI (log2 fold change = 0.428, adjusted $p = 3.29 \times 10^{-6}$), whereas GSE186141 revealed 770 DEGs in OI patients, with 7 overlapping with *PLIN2*-related genes. Notably, *TNFRSF19* (log2 fold change = –2.7454, adjusted $p = 3.930 \times 10^{-7}$ in OI; 1.5001, adjusted $p = 3.482 \times 10^{-3}$ in *PLIN2* knockdown) and *E2F2* (log2 fold change = –2.1428, adjusted $p = 8.830 \times 10^{-5}$ in OI; 1.7207, adjusted $p = 1.244 \times 10^{-2}$ in *PLIN2* knockdown) were identified as key genes. Mendelian randomization analysis confirmed a negative association between *E2F2* and heel BMD ($p = 1.116 \times 10^{-7}$ to 6.073×10^{-5}; effect size –0.0461 to –0.0277).

Conclusions. *PLIN2* and *E2F2* emerge as critical targets for refining MSC therapy in OI, with the potential to improve bone formation and reduce fat accumulation by restoring the osteogenesis–adipogenesis balance. These findings may support the development of combination therapies or engineered MSCs, ultimately improving clinical outcomes for patients with OI.

Key words: Mendelian randomization, lipid metabolism, osteogenesis imperfecta, mesenchymal stem cell therapy, bone homeostasis

Cite as
Wang X, Liu Z, Hu X, Cui Y. Balancing osteogenesis and adipogenesis in isteogenesis imperfecta: *PLIN2* and *E2F2* as key targets for mesenchymal stem cell therapy. *Adv Clin Exp Med*. 2026;35(5):835–846. doi:10.17219/acem/208840

DOI
10.17219/acem/208840

Highlights

- *PLIN2* modulates lipid metabolism and mesenchymal stem cell (MSC) differentiation in osteogenesis imperfecta.
- *E2F2* is a key regulator of bone cell function and bone mineral density.
- Integrated transcriptomic and Mendelian randomization analyses identify *PLIN2* and *E2F2* as therapeutic targets.
- MSC therapy in osteogenesis imperfecta remains limited by variable and transient clinical effects.

Background

Osteogenesis imperfecta (OI) is a genetic disorder characterized by bone fragility and impaired bone formation. This rare connective tissue disorder affects approx. 11.6 per 100,000 pediatric individuals, as reported in a recent nationwide registry study conducted in Turkey (data from 2016–2022).[1] Current treatments for OI primarily rely on bisphosphonates and other antiresorptive agents. Despite these approaches, significant challenges remain, including limited efficacy in severe cases, long-term adverse effects, and the inability to fully restore normal bone quality and reduce fracture risk. Therefore, the identification of novel therapeutic targets remains essential for improving the management of this serious disease. Recent studies have highlighted the complex interplay between glucose and lipid metabolism and bone homeostasis. Notably, hypoglycemic agents such as metformin[2] and glucagon-like peptide-1 (GLP-1) receptor agonists[3,4] have demonstrated potential pro-osteogenic effects, while lipid-lowering agents such as statins[5,6] have also shown promise in promoting bone formation. These findings suggest that targeting glucose and lipid metabolic pathways may provide novel therapeutic strategies for OI.

Recent studies have highlighted the complex interplay between glucose and lipid metabolism and bone homeostasis. Notably, high-fat diet-induced glucose intolerance leads to dysregulated osteoblast lipid metabolism, resulting in reduced bone formation; this effect can be mitigated by enhanced fatty acid oxidation.[7] Furthermore, extracellular metabolites such as lactate, as well as interactions with mesenchymal stromal cells in the tumor microenvironment (TME), exacerbate lipid droplet accumulation in osteosarcoma cells. Targeting PLIN2, a key protein associated with lipid droplet formation, significantly reduces cell viability and increases reactive oxygen species (ROS) production in these cells.[8] PLIN2, a protein involved in lipid droplet formation and fatty acid oxidation, has emerged as a critical regulator in lipid metabolism. Specifically, *PLIN2* knockdown has been shown to induce lipolysis and increase fatty acid oxidation, making it a promising target in various metabolic disorders.[9,10] Given the dynamic relationship between adipogenesis and osteogenesis, and the potential role of *PLIN2* in regulating lipid metabolism and bone cell differentiation, we hypothesize that therapeutic interventions for OI may exert their effects, at least in part, by modulating *PLIN2* expression and thereby influencing the balance between osteogenesis and adipogenesis.

Objectives

This study aims to investigate the therapeutic mechanisms of various interventions for OI by analyzing relevant datasets, with a focus on lipid metabolism-related genes, particularly *PLIN2*, to determine whether they influence the balance between osteoblast and adipocyte differentiation. By elucidating the role of *PLIN2* in OI pathogenesis and therapeutic responses, this study seeks to provide novel insights into potential therapeutic targets for OI.

Materials and methods

Datasets

We retrieved datasets from the Gene Expression Omnibus (GEO; https://www.ncbi.nlm.nih.gov/geo/) database to investigate innovative therapeutic strategies aimed at improving bone health in patients with OI. Among these, mesenchymal stem cell (MSC) therapy has demonstrated potential in clinical settings, with studies showing improvements in bone parameters and stimulation of pro-osteogenic responses (GSE157587), whereas other emerging therapies remain largely limited to animal or cell line models. The dataset GSE214064 examines the impact of *PLIN2* deficiency on hepatic lipid droplet storage and gene expression in fasted mice, demonstrating that *PLIN2* plays a crucial role in regulating lipid droplet size and neutral lipid storage under fasting conditions. The dataset GSE186141 investigates mutations in the *COL1A1* and *COL1A2* genes and their correlation with clinical phenotypes in a Chinese cohort of patients with OI.

The included datasets comprise genome-wide association study (GWAS) summary statistics related to heel bone mineral densite (BMD), derived from the UK Biobank, a large-scale prospective cohort study. Specifically, UKB-b-4657 was designated as the discovery dataset, whereas UKB-b-1096, UKB-b-8875, and UKB-b-20124 served as validation datasets. All datasets originate from a European population, including both males and females, and were generated in 2018.

The variables are continuous and expressed in standard deviations (SD). Sample sizes vary across datasets, ranging from approx. 146,000 to 265,000 individuals, and each dataset includes nearly 9.85 million single-nucleotide polymorphisms (SNPs). These datasets were generated using PHESANT-derived variables from the UK Biobank, based on the hg19/GRCh37 reference genome build. Notably, UKB-b-20124 represents heel BMD T-scores, whereas the remaining datasets correspond to raw BMD measurements.

DEGs analysis methodology

To address the hypothesis that MSC therapy or *PLIN2* deficiency alters gene expression profiles relevant to OI pathophysiology, we employed a dual approach using both the online tool GEO2R (https://www.ncbi.nlm.nih.gov/geo/geo2r) and the R package DESeq2 (v. 3.21.1; https://github.com/thelovelab/DESeq2).[11] DESeq2 models count data using a negative binomial generalized linear model, which accounts for the variance–mean dependence inherent in RNA-seq data and does not assume normality of raw counts. All DESeq2 analyses were performed using standard workflows and default parameters unless otherwise specified. The primary criteria for identifying differentially expressed genes (DEGs) were defined as a log2 fold change >1 or <–1 and an adjusted $p < 0.05$. For multiple testing correction, DESeq2 applies the Benjamini–Hochberg procedure to control the false discovery rate (FDR). However, when these stringent log2 fold change thresholds did not yield any DEGs, the selection criteria were relaxed to include genes with an adjusted $p < 0.05$. This approach ensured the inclusion of potentially relevant genes exhibiting statistically significant differential expression, even with more modest effect sizes.

Data acquisition and preparation

To investigate potential causal relationships between overlapping DEGs identified from OI and *PLIN2*-related gene expression profiles and heel BMD, we performed Mendelian randomization (MR) analysis. We first identified overlapping DEGs from the GSE186141 dataset, which contains gene expression data from patients with OI. These overlapping genes were subsequently analyzed for their association with heel BMD. GWAS summary statistics for heel BMD were obtained from the UK Biobank. One dataset was designated as the discovery dataset, whereas the remaining datasets served as validation datasets. To facilitate efficient retrieval and management of GWAS data, we used the gwasrapidd R package,[12] which enables querying and downloading data from the GWAS Catalog.

MR analysis

To address our hypothesis regarding the causal effects of gene expression on heel BMD, we performed two-sample MR analysis using the TwoSampleMR R package (v. 0.6.17; R Foundation for Statistical Computing, Vienna, Austria).[13] This approach uses genetic variants as instrumental variables to infer causal relationships between exposures (gene expression) and outcomes (heel BMD). For each gene, independent SNPs associated with gene expression were selected as instrumental variables. Instrumental variables were selected based on stringent criteria to ensure validity: SNPs were required to have a $p < 5 \times 10^{-8}$ for association with gene expression and an F-statistic >10 to minimize weak instrument bias. To account for linkage disequilibrium (LD), clumping was performed using PLINK (v. 1.9; https://www.cog-genomics.org/plink) with a 1000 Genomes Project European reference panel, applying an LD r^2 threshold of 0.3 and a clumping window of 1,000 kb to ensure independence of selected SNPs. This procedure reduces multicollinearity among instrumental variables by retaining only independent variants. The inverse variance weighted (IVW) method was used as the primary approach to estimate causal effects, as it provides the most precise estimates when all instrumental variable assumptions are satisfied. This method performs a weighted linear regression of SNP–outcome associations on SNP–exposure associations, with weights inversely proportional to the variance of the SNP–outcome effects. The validity of MR analysis relies on 3 core assumptions for the instrumental variables: 1) relevance (SNPs are associated with the exposure), ensured by the applied p-value and F-statistic thresholds; 2) independence (SNPs are not associated with confounders of the exposure–outcome relationship), supported by the random allocation of genetic variants and further evaluated using MR-Egger regression to detect directional pleiotropy; and 3) exclusion restriction (SNPs influence the outcome only through the exposure), assessed using heterogeneity tests. Regarding the underlying statistical framework, MR assumes linear relationships, homoscedasticity (constant variance of residuals), and normally distributed residuals for valid inference of standard errors (SEs) and p-values. Although these assumptions cannot be directly verified using summary-level data, the application of complementary robust MR methods (e.g., MR-Egger and MR-PRESSO (Mendelian Randomization Pleiotropy RESidual Sum and Outlier)), along with validation across multiple datasets, enhances the robustness of the findings to potential violations. All analyses using the TwoSampleMR package were conducted with default parameters unless otherwise specified.

Statistical analyses and heterogeneity assessment

Causal effects of gene expression on heel BMD were estimated using the IVW method, and statistical significance was assessed using p-values. Heterogeneity among instrumental variables was evaluated using Cochran's Q statistic. Directional pleiotropy was assessed

using MR-Egger regression. Additionally, MR-PRESSO analysis was performed to detect and correct for horizontal pleiotropy.[14] A key consideration in MR analyses based on summary-level data is the potential for bias due to sample overlap between exposure and outcome GWAS datasets or residual linkage disequilibrium if clumping is insufficient. Although strict clumping parameters were applied and findings were validated across multiple UK Biobank datasets to mitigate these concerns, these limitations are inherent to analyses based on summary-level data.

SMR integration

To further validate our findings and integrate GWAS summary statistics with expression quantitative trait loci (eQTL) data, we applied the summary data-based Mendelian randomization (SMR) method using default parameters for heterogeneity ($I^2 < 0.05$ and P_HEIDI > 0.01).[15] SMR enables the identification of candidate genes for complex traits by integrating GWAS summary statistics with eQTL data. Specifically, SMR tests for pleiotropy, whereby a genetic variant influences both gene expression and a complex trait through a shared underlying causal variant. By applying multiple MR approaches and integrating GWAS and eQTL data, we aimed to comprehensively assess potential causal relationships between the identified overlapping DEGs and heel BMD.

Results

DEGs of MSC therapy on OI

Differentially expressed gene analysis was performed using GEO2R based on the GSE157587 dataset, which examines the effects of MSC therapy in OI. This analysis identified a limited set of 4 potentially significant DEGs: *PLIN2*, *PDK4*, *ANGPTL4*, and *HADHA*. Notably, the log2 fold change values for these genes were modest, indicating moderate changes in gene expression. Among the identified DEGs, *PLIN2* showed the most significant adjusted p-value (adjusted $p = 3.290 \times 10^{-6}$), with a corresponding p-value of 1.920×10^{-10}, lfcSE of 0.0673, test statistic of 6.367, log2 fold change of 0.428, and a baseMean of 6529.790 (Table 1).

DEGs analysis of *PLIN2*-deficient mice reveals significant transcriptomic alterations

Differentially expressed gene analysis was conducted on the GSE214064 dataset, which examined gene expression differences between $PLIN2^{+/+}$ and $PLIN2^{-/-}$ mice under 24-h fasting conditions in a *C57BL/6N* background. The analysis aimed to identify *PLIN2*-related genes. Transcriptomic data clearly distinguished the $PLIN2^{+/+}$ and $PLIN2^{-/-}$ sample groups from each other (Fig. 1A). The results revealed 43 downregulated and 102 upregulated

Table 1. Differentially expressed genes (DEGs) following MSC therapy in OI

Gene symbol	GeneID	p_{adj}	p-value	lfcSE	stat	log2FoldChange	baseMean	Description
PLIN2	123	0.001	1.92E-10	0.067	6.367	4.28E-01	6529.790	*PLIN2* (perilipin 2): Perilipin 2, involved in lipid droplet formation and storage, may influence MSC differentiation and lipid metabolism, potentially affecting bone matrix quality and osteoblast function OI following MSC therapy.
PDK4	5166	0.001	4.46E-08	0.164	5.472	8.98E-01	2173.820	PDK4 (pyruvate dehydrogenase kinase 4): Pyruvate dehydrogenase kinase 4, a regulator of glucose and energy metabolism, can modulate the metabolic environment of bone-forming cells, possibly enhancing MSC-mediated repair of defective bone tissue in OI.
ANGPTL4	51129	0.010	1.77E-06	0.142	4.778	6.79E-01	6528.740	ANGPTL4 (angiopoietin like 4): Angiopoietin like 4, known for its role in angiogenesis and lipid metabolism, might contribute to improved vascular support and tissue remodeling in OI, potentially aiding MSC therapy in promoting bone regeneration.
HADHA	3030	0.014	3.20E-06	0.033	4.658	1.51E-01	7701.840	HADHA (hydroxyacyl-CoA dehydrogenase trifunctional multienzyme complex subunit alpha): Hydroxyacyl-CoA dehydrogenase trifunctional multienzyme complex subunit alpha, essential for fatty acid oxidation, may support the energy demands of MSCs during osteogenic differentiation, potentially improving bone strength in OI post-therapy.

Gene symbol – official gene symbol; GeneID – NCBI gene identifier; p_{adj} – adjusted p-value (Benjamini–Hochberg FDR); p-value – raw p-value (Wald test); lfcSE – log2 fold change standard error; stat – Wald statistic; log2FoldChange – log2 fold change (MSC therapy vs control); baseMean – mean of normalized counts across all samples; description – gene name and functional annotation; MSC – mesenchymal stem cells; OI – osteogenesis imperfecta; NCBI – National Center for Biotechnology Information.

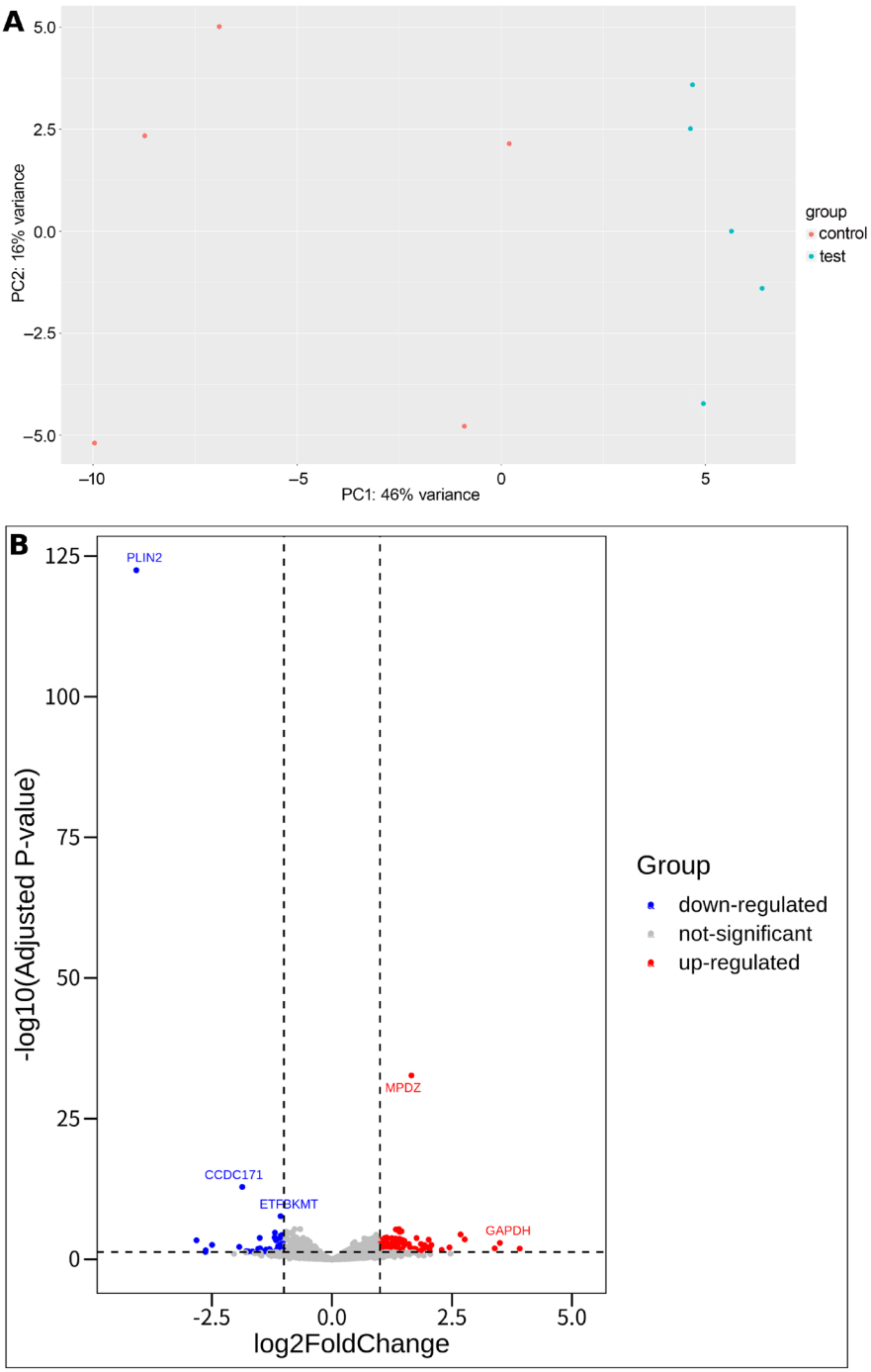

Fig. 1. Differentially expressed genes (DEGs) analysis in *PLIN2*-deficient mice. A. Principal component analysis (PCA) plot of *PLIN2*$^{+/+}$ and *PLIN2*$^{-/-}$ samples based on variance-stabilizing transformation, demonstrating clear separation between groups; B. Volcano plot of DEGs between *PLIN2*$^{+/+}$ and *PLIN2*$^{-/-}$ mice, highlighting significantly upregulated and downregulated genes

DEGs with statistical significance. Among the downregulated genes, *PLIN2* itself exhibited the most substantial log2 fold change, with a value of −4.074 and an adjusted $p = 3.180 \times 10^{-123}$. Other notable downregulated genes included *CCDC171*, *ETFBKMT*, and *CCNG2*, each demonstrating log2 fold changes greater than −1 and adjusted $p < 0.001$. Conversely, the upregulated gene list comprised 102 genes, with *MPDZ* showing the highest log2 fold change of 1.655 and an adjusted $p = 2.100 \times 10^{-33}$. Other significantly upregulated genes included *S100A9*, *ZBP1*, and *CIRBP*, all with log2 fold changes exceeding 1 and adjusted $p < 0.001$ (Fig. 1B).

Overlap of DEGs between OI and *PLIN2*-related gene expression profiles

Differentially expressed gene analysis was performed on the GSE214064 dataset, which examined gene expression differences between *PLIN2*$^{+/+}$ and *PLIN2*$^{-/-}$ mice under 24-h fasting conditions in a *C57BL/6N* background. The analysis aimed to identify *PLIN2*-related genes. Transcriptomic profiling clearly distinguished *PLIN2*$^{+/+}$ and *PLIN2*$^{-/-}$ samples (Fig. 1A). A total of 43 downregulated and 102 upregulated DEGs were identified as statistically significant. Among the downregulated genes, *PLIN2*

exhibited the most substantial log2 fold change (–4.076; adjusted p = 3.180×10^{-123}). Other notable downregulated genes included *CCDC171*, *ETFBKMT*, and *CCNG2*, each with log2 fold change <–1 and adjusted p < 0.001. Conversely, 102 genes were significantly upregulated, with *MPDZ* showing the highest log2 fold change (1.655; adjusted p = 2.100×10^{-33}). Other significantly upregulated genes included *S100A9*, *ZBP1*, and *CIRBP*, all with log2 fold change >1 and adjusted p < 0.001 (Fig. 1B). The overlap between the *PLIN2*-related DEGs and genes previously associated with OI is presented in Table 2.

MR analysis results for overlap of DEGs and heel BMD

Mendelian randomization analysis of *E2F2* was conducted to evaluate its potential causal relationship with heel BMD using UK Biobank data. The UKB-b-4657 dataset served as the discovery dataset, whereas UKB-b-8875, UKB-b-20124, and UKB-b-1096 were used as validation datasets. The IVW method was applied. For each dataset, 29 SNPs were used as instrumental variables. The estimated effect sizes (β coefficients) consistently indicated a negative association between *E2F2* expression and heel BMD, suggesting that increased *E2F2* expression is associated with lower heel BMD. The p-values across all 4 datasets were highly significant, ranging from 1.116×10^{-7} to 6.073×10^{-5}, indicating strong statistical evidence for this association. The 95% confidence intervals (95% CIs) for the effect estimates further supported this finding, as all intervals indicated negative effects across datasets. The corresponding odds ratios (ORs) were close to 1 (0.955–0.973), suggesting that although the association is statistically significant, the magnitude of the effect is relatively small (Table 3, Fig. 2). No other DEGs showed a causal relationship with heel BMD using the IVW method.

Mendelian randomization analysis of the causal relationship between *E2F2* and heel BMD, conducted using the IVW method across 4 UK Biobank datasets (UKB-b-4657, UKB-b-1096, UKB-b-8875, and UKB-b-20124), revealed significant heterogeneity in the causal estimates derived from instrumental SNPs. Specifically, Cochran's Q statistic and the corresponding p-values indicated substantial heterogeneity across all datasets, with Q p-values ranging from 5.140×10^{-17} to 5.895×10^{-13} (Table 4). MR-Egger regression analysis further indicated the presence of directional pleiotropy. This conclusion was supported by statistically significant intercept p-values (p < 0.05) across all datasets, suggesting that genetic variants associated with *E2F2* may influence heel BMD through pathways other than the hypothesized causal mechanism (Table 5).

The MR-PRESSO analysis for horizontal pleiotropy, examining the causal effect of *E2F2* on heel BMD, consistently demonstrated a negative association across all datasets, as indicated by statistically significant p-values (p < 0.001) for the causal estimates. The global test p-value (p_{Glo}), which also remained below 0.001, further supported the overall significance of the observed association (Table 6).

Table 2. Overlap of DEGs between OI and *PLIN2*-related gene

Gene symbol	GeneID	p_{adj}	p-value	lfcSE	stat	log2FoldChange	baseMean	Description
TNFRSF19	55504	0.001	7.48E-10	0.446	–6.156	–2.745	1859.710	tumor necrosis factor (TNF) receptor superfamily member 19
E2F2	1870	0.001	0.001	0.43	–4.985	–2.143	62.150	E2F transcription factor 2
SH3PXD2A	9644	0.001	0.001	0.402	4.498	1.807	6808.540	SH3 and PX domains 2A
MMP11	4320	0.005	0.001	0.492	3.848	1.894	143.030	matrix metallopeptidase 11
TXNIP	10628	0.011	0.001	0.351	3.599	1.263	4511.310	thioredoxin interacting protein
PPP1R3G	648791	0.022	0.001	0.477	3.346	1.595	64	protein phosphatase 1 regulatory subunit 3G
ID3	3399	0.032	0.001	0.369	3.197	1.180	2679.070	inhibitor of DNA binding 3

Gene symbol – official gene symbol; GeneID – NCBI gene identifier; p_{adj} – adjusted p-value (Benjamini–Hochberg false discovery rate); p-value – raw p-value from Wald test; lfcSE – log2 fold change standard error; stat – Wald statistic; log2FoldChange – log2 fold change (experimental vs control); baseMean – mean of normalized counts across all samples; description – gene name and functional annotation; DEGs – differentially expressed genes; OI – osteogenesis imperfecta; NCBI – National Center for Biotechnology Information.

Table 3. Mendelian randomization (MR) analysis results for gene *E2F2* and bone mineral density (BMD) (method – inverse-variance weighted (IVW))

Datasets	nsnp	b	SE	p-value	Lower 95% CI	Upper 95% CI	OR	OR_LCI_95	OR_UCI_95
UKB-b-8875	29.000	–0.028	0.007	0.000	–0.041	–0.014	0.973	0.960	0.986
UKB-b-20124	29.000	–0.028	0.007	0.000	–0.042	–0.015	0.972	0.959	0.986
UKB-b-1096	29.000	–0.034	0.007	0.000	–0.049	–0.020	0.966	0.952	0.981
UKB-b-4657	29.000	–0.046	0.009	0.000	–0.063	–0.029	0.955	0.939	0.971

95% CI – 95% confidence interval; nsnp – number of single nucleotide polymorphisms; b – effect size; SE – standard error of effect size; OR – odds ratio; OR_LCI_95 – odds ratio lower boundary of 95% CI; OR_UCI_95 – odds ratio upper boundary of 95% CI.

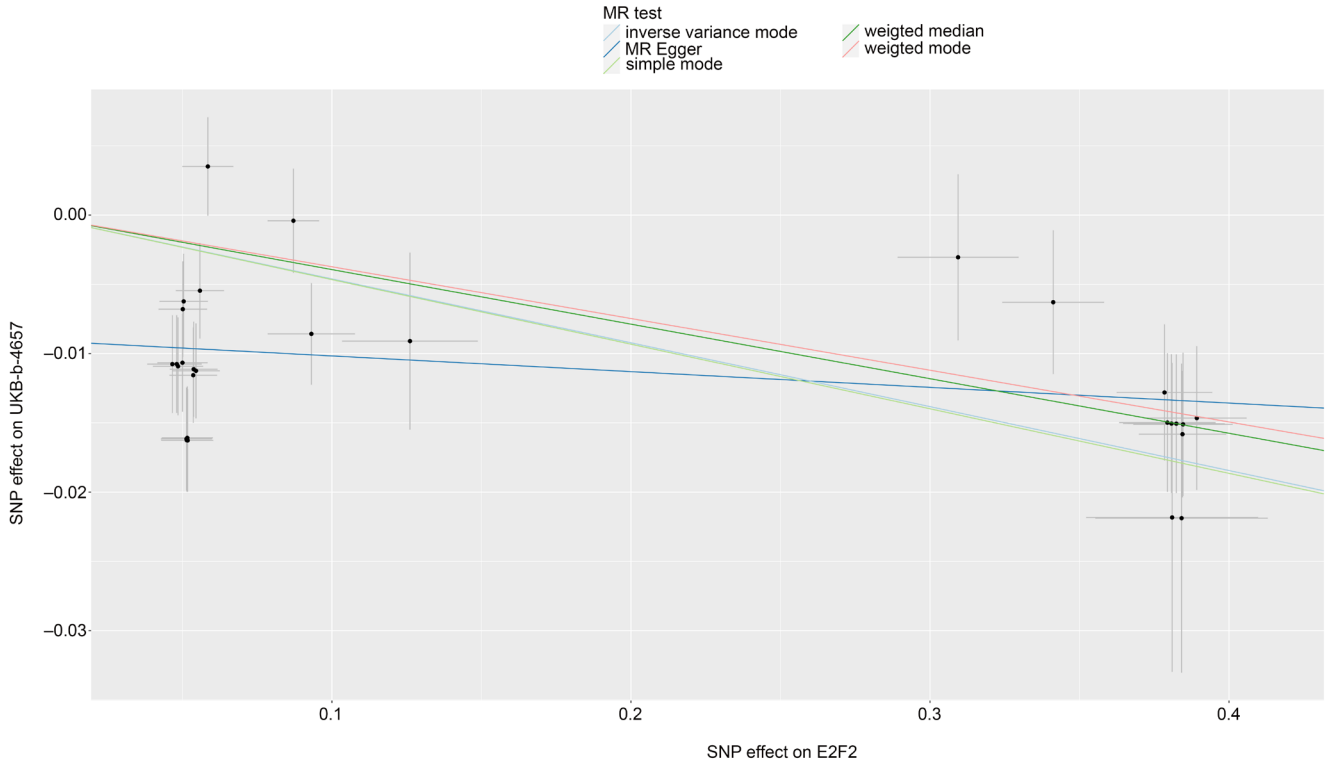

Fig. 2. Scatter plot of Mendelian randomization (MR) analysis for *E2F2* gene in the UKB-b-4657 dataset

Table 4. Heterogeneity analysis results for *E2F2* gene and heel BMD (method – inverse-variance weighted (IVW))

Datasets	Q	Q_df	Q_pval
UKB-b-4657	117.638	28	5.89582E-13
UKB-b-1096	86.642	28	6.57791E-08
UKB-b-8875	135.193	28	5.36E-16
UKB-b-20124	140.945	28	5.14E-17

Datasets – source genome-wide association study (GWAS) dataset identifier; BMD – bone mineral density; method – meta-analysis method (inverse-variance weighted); Q – Cochran's Q statistic; Q_df – degrees of freedom for Cochran's Q statistic; Q_pval – p-value for Cochran's Q statistic.

Table 5. MR-Egger analysis results for *E2F2* gene and heel BMD

Datasets	Egger_ intercept	SE	p-value
UKB-b-4657	−0.009	0.001	2.76E-07
UKB-b-1096	−0.008	0.001	3.52E-08
UKB-b-8875	−0.008	0.001	1.49E-09
UKB-b-20124	−0.008	0.001	1.36E-09

BMD – bone mineral density; SE – standard error of effect size.

Table 6. Horizontal pleiotropy analysis results for *E2F2* gene and heel BMD (MR analysis – raw)

Causal estimate	SD	t-stat	p-value	p_Glo
−0.046	0.009	−5.409	8.15E-06	<0.001
−0.035	0.007	−4.674	6.27E-05	<0.001
−0.028	0.007	−4.061	0.001	<0.001
−0.029	0.007	−4.066	0.001	<0.001

Causal estimate – causal effect estimate (beta coefficient) from MR analysis; SD – standard deviation; t-stat – t-statistic; p-value – p-value for the t-statistic; p_Glo – global p-value for horizontal pleiotropy; horizontal-pleiotropy – pleiotropic effects via independent pathways; MR – Mendelian randomization; raw – unadjusted analysis; BMD – bone mineral density.

Discussion

Our analysis revealed that *PLIN2* is a key gene influenced by MSC therapy in OI, exhibiting the most significant adjusted p-value among the identified DEGs. *PLIN2* plays a critical role in lipid droplet formation and storage, thereby influencing cellular lipid metabolism. Given the important role of lipids in cellular energy homeostasis and signaling, particularly in stem cell differentiation,[16] modulation of *PLIN2* by MSC therapy suggests a potential mechanism for altering the metabolic environment of bone-forming cells in OI. Furthermore, our findings indicate that *PLIN2* deficiency leads to substantial transcriptomic changes, underscoring its regulatory role in gene expression.[17]

The observed interplay between *PLIN2* and other DEGs, such as *TNFRSF19* and *E2F2*, which are significantly downregulated in patients with OI but upregulated under *PLIN2* knockdown conditions, highlights the complex relationship between lipid metabolism and bone homeostasis.[18] This finding suggests that *PLIN2* may act as a key regulator of the balance between osteogenic and adipogenic differentiation of MSCs.[19] Dysregulation of this balance is a hallmark of OI, in which impaired bone formation is often

accompanied by increased adipogenesis.[20] Accordingly, *PLIN2* emerges as a potential therapeutic target in MSC-based therapies for OI, as its modulation may help restore the balance between bone and adipose tissue formation, thereby improving bone matrix quality and osteoblast function. By targeting *PLIN2*, MSC therapy may not only enhance bone repair but also mitigate the adverse effects of excessive adipogenesis, potentially leading to more effective and sustained therapeutic outcomes in patients with OI.[21]

The complex interplay between bone and lipid metabolism is essential for maintaining skeletal health, particularly in conditions such as OI, in which metabolic imbalances may exacerbate disease pathology. Our findings underscore the important role of *PLIN2* in this context, consistent with the broader understanding of how lipid metabolism influences bone homeostasis.[22] The balance between osteogenesis and adipogenesis is tightly regulated, and its disruption can lead to impaired bone quality and increased fracture risk, as observed in OI.[23] The involvement of *PLIN2* in lipid metabolism suggests that it may play a key role in this process, potentially influencing the differentiation of MSCs into either osteogenic or adipogenic lineages. This is particularly relevant in OI, where a shift toward adipogenesis may impair effective bone formation.[24]

Research demonstrates that lipid metabolism is closely linked to bone homeostasis, and disruptions in this balance contribute to OI pathophysiology. For instance, the peroxisome proliferator-activated receptor (PPAR) signaling pathway, a key regulator of adipogenesis and osteogenesis, is influenced by lipid dynamics. Although *PLIN5* has been shown to modulate PPAR signaling in oxidative tissues,[25] the role of *PLIN2* in MSCs and adipocytes suggests that it may indirectly influence this pathway by regulating lipid availability. Specifically, *PLIN2* controls the availability of free fatty acids for energy metabolism compared to their storage within lipid droplets. In OI, where a shift toward adipogenesis is commonly observed, modulation of *PLIN2* may restrict lipid availability for adipogenic pathways and redirect metabolic resources toward osteogenesis. This balance is critical; by optimizing lipid partitioning, *PLIN2* may influence MSC lineage commitment, promoting differentiation toward osteoblasts rather than adipocytes. Bone remodeling involves a tightly regulated interplay between osteoblasts and osteoclasts, with lipid metabolism playing an important regulatory role in this process. Studies indicate that *PLIN5* deficiency alters the expression of osteoclastogenesis-related genes, such as *RANKL* and *OPG*, thereby affecting bone resorption. In contrast, the role of *PLIN2* in lipid storage within the bone microenvironment may indirectly stabilize osteoclast–osteoblast dynamics by modulating the availability of lipid-derived signaling molecules. These molecules, including fatty acids, are known to influence inflammation and oxidative stress – key contributors to the excessive bone fragility observed in OI.[26] Accordingly, the regulation of lipid reserves by *PLIN2* may support bone remodeling processes in the context of MSC-based therapy. The therapeutic relevance of *PLIN2* is further supported by its potential interaction with mitochondrial function, a critical component of energy metabolism in osteoblasts. Previous studies on *PLIN5* have highlighted its role in facilitating mitochondrial lipid utilization, thereby influencing adenosine triphosphate (ATP) production and ROS levels. In OI, mitochondrial dysfunction exacerbates oxidative stress and impairs osteogenesis, and *PLIN5* deficiency may further aggravate these effects. Although *PLIN2* is not directly associated with mitochondria, unlike *PLIN5*, it contributes to cytoplasmic lipid homeostasis and may indirectly support mitochondrial energy supply. This suggests that *PLIN2* could enhance MSC therapy by maintaining the lipid pool required for energy-intensive bone formation.

PLIN2 and *PLIN5*, both members of the perilipin family, exhibit distinct yet complementary roles in lipid and bone metabolism. *PLIN2* primarily regulates lipid droplet storage and hydrolysis in adipocytes and MSCs, whereas *PLIN5*, which is enriched in oxidative tissues, directs lipids toward mitochondria for β-oxidation. In the context of OI, the predominance of *PLIN2* in MSCs positions it as a key regulator of lipid availability, influencing whether these cells differentiate into osteoblasts or adipocytes. In contrast, the mitochondrial role of *PLIN5* supports energy metabolism in active osteoblasts and may help mitigate oxidative stress in OI. The interplay between these proteins is evident: *PLIN2* maintains the lipid reservoir, whereas *PLIN5* facilitates the utilization of these lipids for mitochondrial energy production.

One downstream consequence of the *PLIN2*-mediated inflammatory response is the upregulation of *TNFRSF19*, a member of the tumor necrosis factor (TNF) receptor superfamily. Evidence suggests that *TNFRSF19* expression is elevated under conditions of increased inflammation and cellular stress, potentially as a compensatory response.[27] In the context of *PLIN2* deficiency, increased availability of lipid-derived signaling molecules may stimulate *TNFRSF19*, which has been implicated in the regulation of cell proliferation and survival. Notably, GWAS have identified *TNFRSF19* among candidate genes associated with bone biology, alongside genes such as *PPARG* and *FBN2*.[28] The upregulation of *TNFRSF19* under *PLIN2* knockdown conditions suggests a potential role in osteoblast or pre-osteoblast proliferation, as *TNFRSF19* signaling may promote cell growth in response to inflammatory stimuli. In OI, where bone formation is already impaired, the interplay between *PLIN2* deficiency, inflammation, and *TNFRSF19* upregulation presents a complex scenario. On the one hand, enhanced osteoblast proliferation driven by *TNFRSF19* could potentially improve bone formation and counteract osteopenia. On the other hand, inflammation associated with increased lipid catabolism may offset these benefits by promoting osteoclast activity or impairing bone matrix quality.[29] This dual effect highlights the nuanced role of *PLIN2* as a regulator of both lipid metabolism and inflammatory tone in the bone microenvironment.

The observed upregulation of *TNFRSF19* under *PLIN2* knockdown conditions, as identified in our analysis, further supports its potential role in modulating bone cell dynamics, although the net outcome – whether anabolic or catabolic – likely depends on the balance between these competing processes. From a therapeutic perspective, these findings reinforce the importance of *PLIN2* as a target in MSC-based therapy for OI. Preservation of *PLIN2* function may help mitigate excessive lipolysis and inflammation, thereby limiting downstream activation of *TNFRSF19* and its uncertain effects on bone cell proliferation. Alternatively, if the proliferative effects of *TNFRSF19* prove beneficial, a combined strategy involving *PLIN2* modulation and targeted *TNFRSF19* agonists may enhance osteogenesis while maintaining control over inflammation. This hypothesis is supported by evidence that *TNFRSF19* contributes to bone biology and that *PLIN2* deficiency amplifies inflammatory signaling, underscoring the need for further studies to clarify these interactions.

The downregulation of *E2F2* in OI is consistent with its established role in bone and cartilage biology. *E2F2*, a transcription factor, is involved in cell cycle regulation and differentiation, with studies demonstrating its impact on skeletal tissues. For example, constitutive overexpression of *E2F2* inhibits chondrocyte differentiation and delays endochondral ossification.[30] These findings suggest that reduced *E2F2* expression in OI may reflect impaired chondrocyte or osteoblast differentiation, thereby contributing to the characteristic bone fragility observed in this disease. Conversely, the upregulation of *E2F2* under *PLIN2* knockdown conditions indicates that *PLIN2* may normally suppress *E2F2*, potentially maintaining a balance that favors osteogenesis over excessive proliferation or adipogenesis. This relationship is particularly relevant given the role of *PLIN2* in lipid metabolism, which influences MSC fate. Mechanistically, *E2F2* regulates osteogenesis and adipogenesis through its control of cell cycle progression and progenitor cell proliferation. By governing the transition from proliferation to differentiation, *E2F2* may define the temporal window during which MSCs commit to either osteogenic or adipogenic lineages. In OI, altered *E2F2* expression may disrupt this critical timing, thereby contributing to the imbalance in bone formation. Further evidence supports the therapeutic relevance of *E2F2* in skeletal disorders. In traumatic osteoarthritis, exosomes enriched with miR-125a-5p derived from MSCs target *E2F2* to suppress chondrocyte degeneration, suggesting a protective effect associated with *E2F2* downregulation.[31] Similarly, in osteoarthritis prevention, long noncoding RNA (lncRNA) PTS-1 inhibits *E2F2* via the miR-8085/*E2F2* axis, thereby promoting cartilage homeostasis.[32] These findings contrast with OI, in which *E2F2* downregulation may exacerbate bone defects, highlighting context-dependent effects. In fracture healing, quercetin modulates the miR-6089/*E2F2* axis to enhance osteoblast viability, proliferation, migration, and differentiation,[33] suggesting that increased *E2F2* expression may be beneficial in certain regenerative contexts. The upregulation of *E2F2* following *PLIN2* loss may therefore represent a compensatory mechanism in OI, aimed at enhancing osteoblast activity, although potentially at the expense of increased inflammation or dysregulated differentiation. Mendelian randomization analysis further elucidates the causal relationship between *E2F2* and bone health. Across 4 UK Biobank datasets, *E2F2* expression consistently demonstrated a negative association with heel BMD, with statistically significant p-values (from 1.116×10^{-7} to 6.073×10^{-5}) and effect estimates indicating that higher *E2F2* expression is associated with lower BMD. This finding is consistent with the inhibitory role of *E2F2* in chondrocyte differentiation and suggests that *E2F2* downregulation in OI may represent a compensatory mechanism aimed at preserving BMD, despite the osteopenic phenotype of the disease. However, the relatively small effect sizes (ORs: 0.955–0.973) indicate a modest magnitude of association. Moreover, the presence of significant heterogeneity and directional pleiotropy suggests that additional biological pathways may contribute to this relationship, thereby complicating its potential as a therapeutic target. This heterogeneity indicates that the causal effect estimates across instrumental variables are not fully consistent, which may arise from several factors. Potential explanations include residual confounding, differences in genetic architecture or environmental exposures within UK Biobank subpopulations, and horizontal pleiotropy, whereby SNPs influence the outcome through pathways independent of the exposure. Although MR-Egger and MR-PRESSO analyses were applied to detect and partially account for pleiotropy, residual pleiotropic effects or context-specific genetic interactions may still contribute to the observed variability. These findings suggest that the relationship between *E2F2* and BMD is multifactorial and likely governed by complex biological networks, rather than a single causal pathway. Accordingly, while the MR analysis supports a causal association, the magnitude and generalizability of this effect should be interpreted with caution. Future studies incorporating individual-level data or stratified population analyses are warranted to further elucidate the sources of heterogeneity and refine causal inference.

Mesenchymal stem cell therapy has attracted considerable attention as a potential treatment for OI due to its capacity to differentiate into osteoblasts, home to sites of injury, and exert paracrine effects on recipient tissues. These properties, together with a favorable safety profile, multilineage differentiation potential, low immunogenicity, and relative ease of manufacturing, position MSCs as a promising therapeutic platform for OI. Fetal-derived MSCs, in particular, exhibit enhanced osteogenic potential compared with adult-derived MSCs, as supported by preclinical and early clinical studies demonstrating improved bone formation and potential clinical benefits following intravenous administration.[34] Despite these advantages,

the therapeutic efficacy of MSC therapy in OI remains limited, with outcomes that are often modest, variable, and insufficiently durable, thereby hindering broader clinical translation. Evidence from multiple studies highlights these limitations. Although MSC therapy shows promise, including the superior bone-forming capacity of fetal MSCs, consistent and sustained clinical benefit has not been reliably achieved. More broadly, analyses of clinical-stage MSC therapies indicate that many fail to meet primary efficacy endpoints, suggesting that the intrinsic therapeutic potency of MSCs in humans may be lower than that predicted by preclinical models.[35] This discrepancy may be attributed to heterogeneity arising at multiple stages of cell therapy development, including cell sourcing, expansion, and delivery, all of which can undermine consistency and therapeutic efficacy. In osteoarthritis, MSC injections have been shown to improve clinical outcomes such as pain and joint function; however, magnetic resonance imaging (MRI) typically demonstrates only minimal structural improvement, suggesting that functional benefits may not translate into durable tissue repair.[36] Similarly, clinical trials of MSC therapy in osteoarthritis and rheumatoid arthritis report improvements in joint function, pain reduction, and quality of life without major adverse effects. Nevertheless, the magnitude of these benefits varies, and their long-term durability remains uncertain.[37] Additional challenges include age-related declines in MSC potency and the risk of immune responses associated with allogeneic MSCs.[38] Taken together, these findings indicate that although MSC therapy provides measurable benefits, its effects are often insufficient or unstable for addressing complex underlying pathologies such as OI. Accordingly, the inconsistent and modest efficacy of MSC-based approaches highlights the need to target key regulatory genes, including *PLIN2* and *E2F2*, to enhance osteogenesis and improve therapeutic stability, potentially through combinatorial strategies or MSC engineering.

Future directions and clinical relevance

Our study, primarily computational in nature, identifies *PLIN2* and *E2F2* as promising therapeutic targets in OI and suggests novel strategies to enhance MSC-based therapies by promoting osteogenesis and improving the stability of therapeutic outcomes. Future research should prioritize experimental validation of these findings using both in vitro and in vivo models to confirm the causal roles of *PLIN2* and *E2F2* in osteoblast and adipocyte differentiation. Further investigation into the molecular mechanisms by which modulation of these genes affects bone quality and fracture healing is warranted. Ultimately, these insights may facilitate the development of more targeted and effective MSC-based interventions for OI, supporting the advancement of personalized therapeutic approaches aimed at optimizing bone health and reducing disease burden.

Limitations of the study

Although our bioinformatics analysis provides valuable insights into the roles of *PLIN2* and *E2F2* in OI and their potential as therapeutic targets, it is inherently limited by its reliance on computational methods and publicly available datasets. The identification of DEGs and the causal associations inferred from MR analyses are based on statistical relationships rather than direct experimental evidence, and therefore should be interpreted with caution.

Factors such as sample heterogeneity, batch effects, and unmeasured confounders may have influenced the observed expression patterns and associations. Moreover, the upregulation of *E2F2* and *TNFRSF19* under *PLIN2* knockdown conditions, contrasted with their downregulation in OI, suggests a complex regulatory interplay that requires functional validation. Further experimental studies – including in vitro assays using MSC models, in vivo *PLIN2* knockout models, and histological analyses of bone formation – are necessary to elucidate the mechanistic role of *PLIN2* in lipid metabolism and the impact of *E2F2* on osteoblast differentiation and BMD. In addition, clinical translation will require well-designed trials to evaluate the feasibility and efficacy of targeting these pathways in MSC-based therapies, ensuring that bioinformatics-derived hypotheses are validated by robust experimental and clinical evidence.

Conclusions

Our study highlights the pivotal role of *PLIN2* in regulating lipid metabolism and MSC fate in OI, with *E2F2* emerging as a key downstream regulator that influences bone cell dynamics and BMD. The overlap of DEGs between OI and *PLIN2*-related profiles, together with MR evidence linking *E2F2* to skeletal traits, underscores their therapeutic relevance. Despite the promise of MSC-based therapies for OI, their efficacy remains modest and variable, characterized by transient clinical benefits, inconsistent outcomes, limited structural repair, and potential immunological challenges. These limitations highlight the need for more targeted and mechanistically informed approaches. We propose that *PLIN2* and *E2F2* represent critical molecular targets for enhancing MSC therapy. Precise modulation of *PLIN2* to optimize lipid metabolism, together with regulation of *E2F2*-mediated differentiation pathways, may improve osteogenic potential and promote more durable therapeutic effects. Although these findings provide a compelling framework, experimental and clinical validation is essential to translate bioinformatics-driven insights into effective therapeutic strategies, ultimately improving skeletal outcomes in patients with OI.

Data Availability Statement

All data used in this study are derived from publicly available repositories. This study analyzed datasets from the Gene Expression Omnibus (GEO; GSE157587, GSE214064, GSE186141) and UK Biobank genome-wide association study (GWAS) summary statistics (UKB-b-4657, UKB-b-1096, UKB-b-8875, UKB-b-20124).

Consent for publication

Not applicable.

Use of AI and AI-assisted technologies

Not applicable.

ORCID iDs

Xishun Wang https://orcid.org/0009-0001-9537-6953
Zhenjiang Liu https://orcid.org/0000-0003-2635-191X
Xinyong Hu https://orcid.org/0009-0009-0582-3878
Yinpeng Cui https://orcid.org/0000-0002-2070-6057

References

1. Görgün B, Yaşar NE, Bingöl İ, et al. Prevalence, number of fractures, and hospital characteristics among the pediatric population with osteogenesis imperfecta: Results from the nationwide registry of Türkiye. *J Pediatr Orthop B*. 2025;34(3):249–256. doi:10.1097/BPB.0000000000001192
2. Carbine KA, Larson MJ. Quantifying the presence of evidential value and selective reporting in food-related inhibitory control training: A *p*-curve analysis. *Health Psychol Rev*. 2019;13(3):318–343. doi:10.1080/17437199.2019.1622144
3. Andreotti JP, Lousado L, Magno LAV, Birbrair A. Hypothalamic neurons take center stage in the neural stem cell niche. *Cell Stem Cell*. 2017;21(3):293–294. doi:10.1016/j.stem.2017.08.005
4. Wagenlehner FME, Naber KG. Cefiderocol for treatment of complicated urinary tract infections. *Lancet Infect Dis*. 2019;19(1):22–23. doi:10.1016/S1473-3099(18)30722-9
5. Gargioli C, Slack JMW. Cell lineage tracing during *Xenopus* tail regeneration. *Development (Camb)*. 2004;131(11):2669–2679. doi:10.1242/dev.01155
6. Glatard T, Montagnat J, Pennec X. Medical image registration algorithms assesment: Bronze Standard application enactment on grids using the MOTEUR workflow engine. *Stud Health Technol Inform*. 2006;120:93–103. PMID:16823126.
7. Nandy A, Helderman RCM, Thapa S, et al. Enhanced fatty acid oxidation in osteoprogenitor cells provides protection from high-fat diet induced bone dysfunction. *J Bone Miner Res*. 2025;40(2):283–298. doi:10.1093/jbmr/zjae195
8. Cortini M, Ilieva E, Massari S, Bettini G, Avnet S, Baldini N. Uncovering the protective role of lipid droplet accumulation against acid-induced oxidative stress and cell death in osteosarcoma. *Biochim Biophys Acta Mol Basis Dis*. 2025;1871(2):167576. doi:10.1016/j.bbadis.2024.167576
9. Angelini G, Panunzi S, Pompili M, et al. Performance of noninvasive tests for metabolic dysfunction-associated steatohepatitis and liver fibrosis resolution after bariatric surgery. *Clin Chem*. 2025;71(3):406–417. doi:10.1093/clinchem/hvae208
10. Deng X, Liu H, Zhao W, et al. Expression of AMPK and *PLIN2* in the regulation of lipid metabolism and oxidative stress in bitches with open cervix pyometra. *BMC Vet Res*. 2025;21(1):164. doi:10.1186/s12917-025-04622-1
11. Love MI, Huber W, Anders S. Moderated estimation of fold change and dispersion for RNA-seq data with DESeq2. *Genome Biol*. 2014;15(12):550. doi:10.1186/s13059-014-0550-8
12. Magno R, Maia AT. gwasrapidd: An R package to query, download and wrangle GWAS catalog data. *Bioinformatics*. 2020;36(2):649–650. doi:10.1093/bioinformatics/btz605
13. Hemani G, Zheng J, Elsworth B, et al. The MR-Base platform supports systematic causal inference across the human phenome. *eLife*. 2018;7:e34408. doi:10.7554/eLife.34408
14. Verbanck M, Chen CY, Neale B, Do R. Detection of widespread horizontal pleiotropy in causal relationships inferred from Mendelian randomization between complex traits and diseases. *Nat Genet*. 2018;50(5):693–698. doi:10.1038/s41588-018-0099-7
15. Zhu Z, Zhang F, Hu H, et al. Integration of summary data from GWAS and eQTL studies predicts complex trait gene targets. *Nat Genet*. 2016;48(5):481–487. doi:10.1038/ng.3538
16. Tsai TH, Chen E, Li L, et al. The constitutive lipid droplet protein *PLIN2* regulates autophagy in liver. *Autophagy*. 2017;13(7):1130–1144. doi:10.1080/15548627.2017.1319544
17. Wu Y, Chen K, Li L, et al. *PLIN2*-mediated lipid droplet mobilization accelerates exit from pluripotency by lipidomic remodeling and histone acetylation. *Cell Death Differ*. 2022;29(11):2316–2331. doi:10.1038/s41418-022-01018-8
18. Kaushik S, Cuervo AM. AMPK-dependent phosphorylation of lipid droplet protein *PLIN2* triggers its degradation by CMA. *Autophagy*. 2016;12(2):432–438. doi:10.1080/15548627.2015.1124226
19. Luo H, She X, Zhang Y, et al. *PLIN2* promotes lipid accumulation in ascites-associated macrophages and ovarian cancer progression by HIF1α/SPP1 signaling. *Adv Sci (Weinh)*. 2025;12(12):2411314. doi:10.1002/advs.202411314
20. Li Y, Khanal P, Norheim F, et al. *PLIN2* deletion increases cholesteryl ester lipid droplet content and disturbs cholesterol balance in adrenal cortex. *J Lipid Res*. 2021;62:100048. doi:10.1016/j.jlr.2021.100048
21. Mardani I, Tomas Dalen K, Drevinge C, et al. *PLIN2*-deficiency reduces lipophagy and results in increased lipid accumulation in the heart. *Sci Rep*. 2019;9(1):6909. doi:10.1038/s41598-019-43335-y
22. Kong L, Zhao H, Wang F, et al. Endocrine modulation of brain-skeleton axis driven by neural stem cell-derived perilipin 5 in the lipid metabolism homeostasis for bone regeneration. *Mol Ther*. 2023;31(5):1293–1312. doi:10.1016/j.ymthe.2023.02.004
23. Zhang J, Hu W, Zou Z, et al. The role of lipid metabolism in osteoporosis: Clinical implication and cellular mechanism. *Genes Dis*. 2024;11(4):101122. doi:10.1016/j.gendis.2023.101122
24. Peng H, Hu B, Xie LQ, et al. A mechanosensitive lipolytic factor in the bone marrow promotes osteogenesis and lymphopoiesis. *Cell Metab*. 2022;34(8):1168–1182.e6. doi:10.1016/j.cmet.2022.05.009
25. Xiao H, Li W, Qin Y, et al. Crosstalk between lipid metabolism and bone homeostasis: Exploring intricate signaling relationships. *Research (Wash D C)*. 2024;7:0447. doi:10.34133/research.0447
26. Dai B, Xu J, Li X, et al. Macrophages in epididymal adipose tissue secrete osteopontin to regulate bone homeostasis. *Nat Commun*. 2022;13(1):427. doi:10.1038/s41467-021-27683-w
27. Qiu W, Hu Y, Andersen TE, et al. Tumor necrosis factor receptor superfamily member 19 (*TNFRSF19*) regulates differentiation fate of human mesenchymal (stromal) stem cells through canonical Wnt signaling and C/EBP. *J Biol Chem*. 2010;285(19):14438–14449. doi:10.1074/jbc.M109.052001
28. Pei YF, Liu L, Liu TL, et al. Joint association analysis identified 18 new loci for bone mineral density. *J Bone Miner Res*. 2019;34(6):1086–1094. doi:10.1002/jbmr.3681
29. Mekchay S, Pothakam N, Norseeda W, et al. Association of *IFNA16* and *TNFRSF19* polymorphisms with intramuscular fat content and fatty acid composition in pigs. *Biology (Basel)*. 2022;11(1):109. doi:10.3390/biology11010109
30. Scheijen B, Bronk M, Van Der Meer T, Bernards R. Constitutive E2F1 overexpression delays endochondral bone formation by inhibiting chondrocyte differentiation. *Mol Cell Biol*. 2003;23(10):3656–3668. doi:10.1128/MCB.23.10.3656-3668.2003
31. Xia Q, Wang Q, Lin F, Wang J. miR-125a-5p-abundant exosomes derived from mesenchymal stem cells suppress chondrocyte degeneration via targeting *E2F2* in traumatic osteoarthritis. *Bioengineered*. 2021;12(2):11225–11238. doi:10.1080/21655979.2021.1995580
32. Ma C, Chen Q, Wei YF, et al. LncRNA PTS-1 protects against osteoarthritis through the *miR-8085/E2F2* axis. *J Inflamm Res*. 2025;18:347–366. doi:10.2147/JIR.S496185

33. Dong R, Liu MY, Zhu GB, Tan KM, Wang YQ, Li L. Modulation of the microRNA-6089/E2F transcription factor2 axis by querceting: Implications for osteoblast viability, proliferation, migration, and osteogenic differentiation in fracture healing. *J Physiol Pharmacol*. 2024;75(2):173–183. doi:10.26402/jpp.2024.2.06
34. Götherström C, Walther-Jallow L. Stem cell therapy as a treatment for osteogenesis imperfecta. *Curr Osteoporos Rep*. 2020;18(4):337–343. doi:10.1007/s11914-020-00594-3
35. Levy O, Kuai R, Siren EMJ, et al. Shattering barriers toward clinically meaningful MSC therapies. *Sci Adv*. 2020;6(30):eaba6884. doi:10.1126/sciadv.aba6884
36. Fuggle NR, Cooper C, Oreffo ROC, et al. Alternative and complementary therapies in osteoarthritis and cartilage repair. *Aging Clin Exp Res*. 2020;32(4):547–560. doi:10.1007/s40520-020-01515-1
37. Hwang JJ, Rim YA, Nam Y, Ju JH. Recent developments in clinical applications of mesenchymal stem cells in the treatment of rheumatoid arthritis and osteoarthritis. *Front Immunol*. 2021;12:631291. doi:10.3389/fimmu.2021.631291
38. Bagge J, Freude K, Lindegaard C, Holst B, Hölmich P. Pros and cons of using autologous versus allogenic stem cells for the treatment of osteoarthritis [in Danish]. *Ugeskr Læger*. 2024;186(1):V06230423. doi:10.61409/V06230423